

Dimensions of Neuronal Nicotinic Acetylcholine Receptor Channel As Estimated from the Analysis of the Channel-Blocking Effects

S. Kertser, A. Bobryshev, S. Voitenko, V. Gmiro*, N. Brovtsyna**, V. Skok

Bogomoletz Institute of Physiology, Kiev-24, Ukraine

Received: 22 October 1997/Revised: 9 February 1998

Abstract. Acetylcholine-induced membrane currents and excitatory postsynaptic currents (EPSCs) were recorded from the neurons of rat superior cervical ganglion (SCG) using the whole-cell patch clamp and the two-electrode voltage clamp techniques, correspondingly. The EPSC decay was bi-exponential, with fast and slow components characterized by time constants 5.5 ± 0.5 msec and 20.4 ± 1.2 msec (mean \pm SEM; $n = 23$), respectively. Blocking of these currents by a series of newly synthesized *bis*-cationic ammonium compounds, the pentamethonium and pentaethonium derivatives, was analyzed. Blocking effects were due to a block of nicotinic acetylcholine receptor (nAChR) open channel, with mean blocker binding rate constants for the fast component three to five times higher than those for the slow component. Dimensions of a nAChR ionic channel were deduced from a relationship between blocking activity of the compounds and the size of the projections of their three-dimensional molecular models on the neuronal membrane plane. The results suggest that there are two populations of nAChRs in rat SCG neurons; while these populations differ in the rate constants of the binding by the blocker to their open channels, they exhibit similar channel diameter, 11.8 Å, at the level at which the blockers bind to the channel.

Key words: Neuronal nicotinic receptor — Ionic channel — Open channel block — Sympathetic ganglion

* Present address: Institute of Experimental Medicine, St. Petersburg, A-22, Russia

** Present address: Sechenov Institute of Evolutionary Physiology and Biochemistry, St. Petersburg, K-223, Russia

Correspondence to: V. Skok

Introduction

Recent studies suggest that ionic channel of nicotinic acetylcholine receptor (nAChR) of the *Torpedo* electric organ and the frog endplate is a funnel-shaped pore (Changeux et al., 1992; Vidal & Changeux, 1996; Unwin, 1993, 1995) with the cross-profile in its most narrow part (selectivity filter) being a rectangle of 6.5×6.5 Å (Dwyer et al., 1980; Hille, 1984). Neuronal nAChRs are much more diverse in their subunit composition, than those of the muscle and the electric organ (Steinbach & Ifune, 1989; Boulter et al., 1990; Luetje & Patrick, 1991; Albuquerque et al., 1995; Lindstrom, 1996), and, particularly, in their channel-lining domains (Role, 1992; Bertrand et al., 1993). Altogether, the channel architecture in neuronal nAChRs still remains poorly understood.

Neuronal nAChRs are much more sensitive than the nAChRs of skeletal muscle fibers and electric organ, to blocking action of *bis*-quaternary ammonium compounds which is due to open channel-blocking mechanism (Ascher, Large & Rang, 1979; Gurney & Rang, 1984; Skok, Selyanko & Derkach, 1989). On the basis of the relationship between the size of the channel-blocking molecules and their blocking activity it was proposed that the blocking molecules interact with the nAChR channel of the rat superior cervical ganglion (SCG) neurons at the level where its cross-profile is that of a rectangle of 6.1×8.3 Å (Zhorov et al., 1991; Skok, 1992; Brovtsyna, Magazanik & Zhorov, 1996); it was also suggested that a selectivity filter, with the cross-profile of 5.8×8.0 Å, is located between that level and cytoplasmic end of the channel (Skok et al., 1995). These results were advanced assuming that the blocking molecule adopts an extended conformation perpendicular to the membrane.

It should be noted that the blocking molecule may approach the channel at any orientation, not only with its longitudinal axis perpendicular to the cell membrane.

The latter case is apparently most probable for a relatively narrow part of the channel, whereas a random orientation is most probable for the channel entrance, where the channel diameter is larger than in its deeper portions. A study of a relationship between the channel-blocking activity and the projections of the blocking molecules on the channel at *any* orientation of the molecule may thus allow one to estimate the dimensions of a new channel portion, of larger diameter, and, possibly, less deeply located, as compared with that investigated earlier. This was the aim of the present work.

Materials and Methods

RECORDING PROCEDURE

The SCG of the rat was isolated under ether anesthesia. In one series of experiments, the ganglion was incubated for about one hour at 37°C in a solution containing 0.4% collagenase (Sigma type 1A). The solution was of the following composition (mM): NaCl, 133; KCl, 5.9; CaCl₂, 2.5; MgCl₂, 1.2; Tris-HCl, 10; glucose, 11 (pH 7.4). The ganglion was then fixed with small pins to the Sylgard-covered bottom of the perspex chamber, and continuously perfused with a solution of the above composition (without collagenase) at room temperature (20–24°C). Membrane currents were induced in the neurons by acetylcholine (ACh) applied ionophoretically through an extracellular micropipette under visual control with Nomarski optics. Acetylcholine-induced membrane currents (ACh currents) were recorded using the whole-cell patch-clamp recording method. The recording micropipette was filled with a solution of the following composition (mM): NaCl, 140; CaCl₂, 1.0; EGTA, 11; HEPES, 10 (pH 7.2); the solution was potassium-free to prevent the appearance of muscarinic ACh currents, only the nicotinic currents remaining present. The currents were recorded at a frequency band of 0–1.0 kHz.

Blocking agents used as tools to measure the nAChR channel dimensions, were applied through the perfusion solution, and their blocking activities were estimated as inverse IC₅₀s, the concentrations needed to reduce the amplitude of the control ACh current by 50% (Table 1).

In the second series of experiments the isolated rat SCG was not treated with collagenase, and, instead of ACh currents, the excitatory postsynaptic currents (EPSCs) evoked by single electrical stimuli applied to the cervical sympathetic nerve were recorded with a conventional two-electrode recording technique. For more details on the methods used, *see* Voitenko, Bobryshev & Skok, 1993.

DRUGS

The *bis*-cationic ammonium compounds used as blocking agents were the pentamethonium and pentaethonium derivatives synthesized as dibromides in the Institute of Experimental Medicine, Russian Academy of Medical Sciences, St. Petersburg. Their chemical structures are shown in Table 1.

THE SIZES OF THE BLOCKING MOLECULES AND THEIR PROJECTIONS

Three-dimensional models of the blocking molecules were constructed using an OUR Molecular Modeling Package computer program

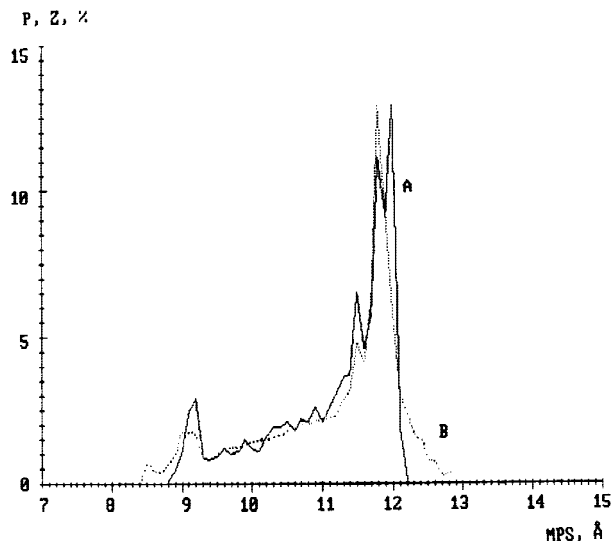


Fig. 1. Probability spectra of maximum projection sizes (MPSs) for a single conformer (A) and for the conformer-containing compound VII (B; *see* Table 1). The MPS probabilities (P, Z) (*ordinate*) are plotted against the corresponding MPSs (*abscissa*). Total probability of all MPSs of a conformer or a compound equals to 100%. In B, the MPS probabilities of each conformer were multiplied by the probability of the conformer existence within the compound and summated.

(Vinter, Davis & Saunders, 1987), taking into account the valences and bonds between atoms. The initial parameters (bond length, distances and angles between the atoms) were taken arbitrarily. By changing the initial parameters, the three-dimensional location of atoms in the molecule which corresponded to its minimum energy, could be calculated by means of the OUR program. Thus, final coordinates of the atoms and the energy of one of the conformers (stable conformations) of the molecule were determined. A similar procedure was performed to find the atoms' coordinates and energy for other conformers of the molecule. This procedure was repeated until new conformers appeared to be similar to those found earlier. Only the conformers whose energy was lower than 3.0 kcal/mol were considered.

Because each conformer projection on a membrane plane is of a complex shape, while only its maximum size is crucial for entering the channel of a certain diameter, only the maximum size of each projection (referred to below as a "maximum projection size", MPS) was further considered. The MPS was a distance between the two hydrogen atoms of the molecule projection most remote from each other, calculated up to 0.1 Å, plus two Van-der-Vaals radii, each equal to 1.2 Å.

The MPS probability spectrum was then constructed. In the spectrum, the probability of a realization of each MPS in % (*ordinate*) was plotted against the corresponding MPSs scaled at 0.1 Å step (*abscissa*). The probability of a realization of each MPS (referred to as "MPS probability") was determined as a ratio between the number of particular MPS that was obtained during the arbitrary rotating of a conformer model around all three axes, and the total number of the turns (Giles, 1985). Rotating was continued until a stable spectrum, with the changes of the MPS probability not exceeding 0.1% after 1,000 turns, was obtained (about 10,000 turns were generally required to reach stability). All MPS found varied from 7.7 to 14.6 Å.

Figure 1A, shows an example of a MPS probability spectrum for one of conformers of the blocking compound VII shown in Table 1 (this compound was more active than any other compound tested). Total probability of all MPSs of a conformer was 100%. The two

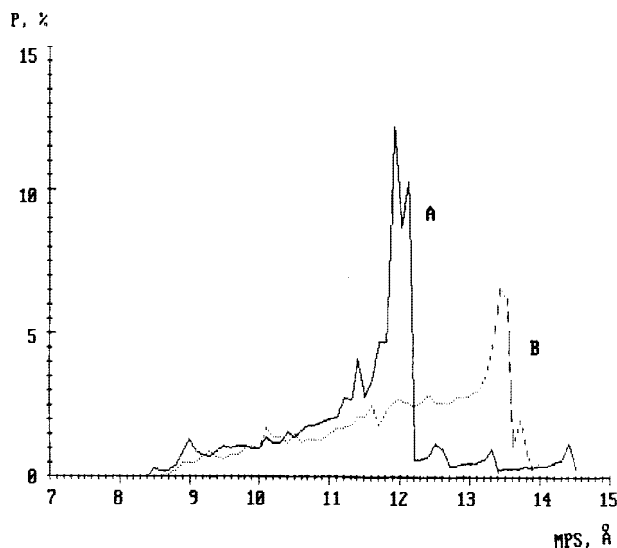


Fig. 2. Same as in Fig. 1 B, but for two other compounds, IV (A) and XIII (B) (see Table 1).

largest probability peaks (12.8% and 11.2%) correspond to MPSs equal to 12.0 and 11.8 Å, respectively (see Fig. 1A).

Next step was to obtain the MPS probability spectrum of the compound. This spectrum was accomplished by summing up the MPS probability spectra of all conformers of this particular compound, taking into account the probability of an existence of the conformer itself; the following equation was used:

$$P = \sum_{k=1}^m Z_k C_k, \quad (1)$$

where P is the MPS probability of the compound, m is the number of conformers of the compound, Z_k is the MPS probability for the conformer k of the compound, and C_k is the probability of the existence of the conformer k calculated from the following equation (Zhorov et al., 1991):

$$C_k = \frac{\exp(-E_k/RT)}{\sum_{k=1}^m \exp(-E_k/RT)}, \quad (2)$$

where R is the universal gas constant, T is temperature taken as 300°K, m is the number of the conformers of the compound, and E_k is the energy of the conformer k .

An example of the MPS probability spectrum for the compound VII (Table 1) is shown in Fig. 1 (B). The peak at the MPS 11.8 Å is the highest for the compound (12.8%). For comparison, the MPS probability spectra for two more compounds, IV and XIII (Table 1), are shown (see Fig. 2A and B, respectively). Note that the MPS for the peaks in the MPS probability spectrum of a compound IV, which is much more active than the compound XIII (see Table 1), are very close to the peak of the compound VII shown in Fig. 1B; these peaks are not present in the case of compound XIII.

The MPS probability spectra were constructed for each of the 15 blocking compounds shown in Table 1, and were used to evaluate the nAChR channel diameter.

Results

BLOCKADE OF ACh CURRENTS

Frames A 1 and 2 of Fig. 3 illustrate the examples of the ACh currents recorded from a neuron of rat SCG at -110 mV membrane potential level in normal Krebs solution, and in the presence of blocking compound II (Table 1), respectively. The records shown in frames A 3 and 4 of Fig. 3 were obtained at -50 mV membrane potential. As shown in the frame B of Fig. 3, the blocking effect is strongly voltage-dependent. When the extent of block is expressed as $I/I_B - 1$, where I and I_B stand for the amplitudes of the ACh currents recorded in the absence and in the presence of a blocker, correspondingly, the block at -50 mV is only 0.63 of that at -110 mV. All 15 blocking compounds tested produced voltage-dependent blocking effects. Their $1/IC_{50}$ values obtained at -50 mV membrane potential are shown in Table 1.

BLOCKADE OF EPSC

A decay of the EPSC recorded in normal solution can be described by two exponentials, fast and slow, with the time constants τ_f and τ_s . In the case of the EPSC shown in Fig. 3C, these constants equal 6.6 and 28.6 msec, respectively; Fig. 3C illustrates fit for only the slow exponential, the fast component being left unfitted. The mean values of τ_f and τ_s obtained from 23 neurons of rat SCG at -50 mV holding potential were equal to 5.5 ± 0.5 ms and 20.4 ± 1.2 msec ($n = 23$), respectively. It should be noted that the constants τ_f and τ_s revealed a weak but significant correlation (a correlation coefficient, R , was 0.64; $P > 0.99$).

The blocking compounds tested (Table 2) reduced the EPSC amplitude and shortened the EPSC decay time course in a voltage-dependent manner. As illustrated in Fig. 3D, at the concentration of 4×10^{-5} M of compound IV the time constants of the fast and slow components were reduced from 9.2 and 24.4 msec to 5.5 and 12.0 msec, respectively. The rate constant k^*_{+B} of a blocker binding to the open nAChR channel was calculated from the equation $k^*_{+B} = [(\tau')^{-1} - \tau^{-1}]X_B^{-1}$, where τ and τ' stand for the EPSC decay time constants measured in normal solution and in the presence of a blocker, respectively, and X_B is concentration of the blocker (Colquhoun, Ogden & Mathie, 1987). The k^*_{+B} values calculated for the fast and slow components of the EPSC decay, k^*_{+Bf} and k^*_{+Bs} , for six blocking compounds, are shown in Table 2. The blockers listed in Table 2 have been chosen from those shown in Table 1 as exhibiting statistically different $1/IC_{50}$ values estimated from a blocker-induced decrease of ACh currents, except for the pairs I–IV and I–XV (for more detailed analysis of the data shown in Table 2 see below). The k^*_{+Bf} and k^*_{+Bs}

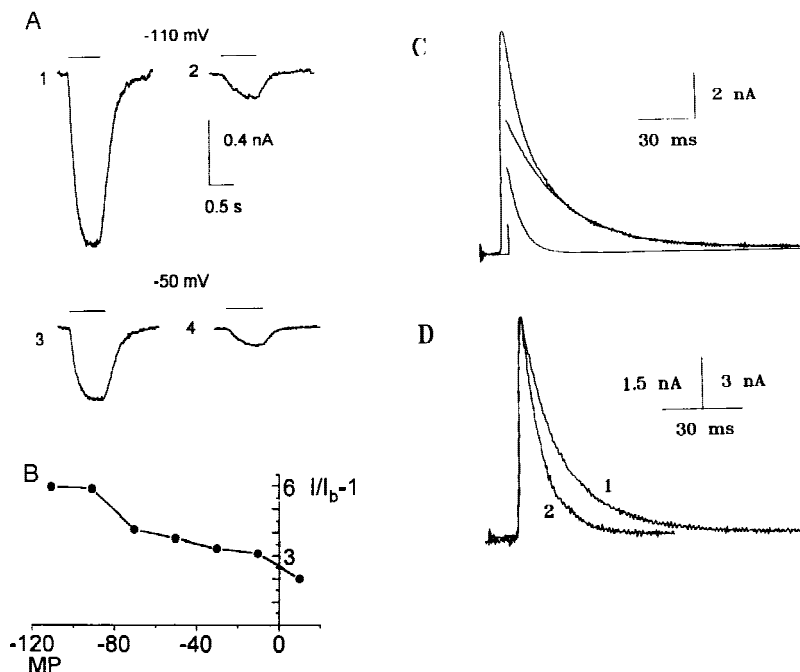


Fig. 3. Blocking effects of compounds II (A, B) and IV (D) (see Table 1) on nAChRs of rat superior cervical ganglion neurons. (A) Membrane currents recorded in normal solution (1, 3), and in the presence of a 1×10^{-6} M concentration of compound II (2, 4), at -110 mV (1, 2) and -50 mV (3, 4). Horizontal bars indicate the time of ACh application. (B) Voltage dependence of the blocking effect expressed as $I/I_B - 1$, where I and I_B stand for the amplitudes of the membrane currents recorded in the absence and in the presence of a blocker, correspondingly. (C) Excitatory postsynaptic current (EPSC) recorded in normal solution; the trace shown is an average of 40 original traces. An EPSC decay phase was fitted by single exponential with a time constant of the slow EPSC component, τ_s , equal to 28.6 msec. Subtraction of this component from the original EPSC revealed one more, fast EPSC decay component, with a time constant, τ_f , equal to 6.6 msec. (D) The EPSCs recorded in normal solution (1) and in the solution containing 4×10^{-5} M concentration of compound IV (2). The blocking compound reduced τ_f and τ_s from 9.2 and 24.4 msec (1) to 5.5 and 12.0 ms (2), respectively. Note that the amplitude calibration scales for 1 and 2 are different, to make the EPSC amplitudes equal to each other. The current traces in 1 and 2 are averages from 4 and 20 original traces, respectively. Holding membrane potential in C and D was -50 mV. The records A, B, C and D were obtained from four different neurons, respectively.

values shown in Table 2 correlate with the blocking activities of the corresponding compounds, $1/IC_{50}$ ($R = 0.94$; $P > 0.99$).

Voltage dependence of the blocking effect on ACh current and the blocker-induced reduction of the EPSC decay time constant are typical of the open channel block (Adams, 1976; Colquhoun et al., 1987); this indicates that the open channel blocking mechanism is involved in the blocking effects of the compounds used in this work. The fact that the $1/IC_{50}$ estimates correlate with the rate constants of the blockers binding to the open channel suggests that open channel-blocking mechanism is involved, rather than any other blocking mechanism, e.g., competitive block or desensitization. This is consistent with the finding that ganglion-blocking activities of bis-cationic ammonium compounds correlate with their k_{+B}^* values (Skok, Selyanko & Derkach, 1983; Skok et al., 1989).

CHANNEL DIMENSIONS

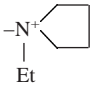
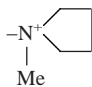
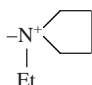
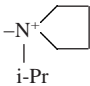
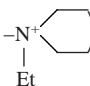
It was assumed that, to attain maximum blocking effect, a blocking molecule should be accommodated within the channel at the level where it binds to the channel wall, thus plugging the channel. Accordingly, the blocking activity of a compound depends on the number of its

molecules that reach the channel level in question. The channel diameter at the site of binding can be therefore estimated as equal to the value of the MPS at which the highest blocking activity of the compounds tested is observed; or, alternatively, this estimate is indicated as the best correlation between blocking activity and the MPS probability among the compounds tested. Accordingly, two different approaches were used to find this MPS. With regard to the first approach, the difference P_d between the weighted and non-weighted MPS probability spectra for the 15 blocking compounds tested was calculated and normalized to 100%. The weighted MPS probability for each blocking compound was found by multiplying its non-weighted MPS probability spectrum, P_p , by blocking activity of the compound relative to the blocking activity of the compound XIII as the least potent one (for examples of P_p s, see Figs. 1B and 2A and B):

$$P_d = \sum_{i=1}^{15} P_i (1/IC_{50(i)} - 1) \quad (3)$$

Figure 4 shows the P_d spectrum; a peak corresponding to the MPS of 11.8 \AA may be noted. Therefore, the MPS value equal to 11.8 \AA corresponds to the maximum blocking activity of the blocking compounds tested. It can be seen, from analyzing the P_d spectra for each blocking compound, that the peak shown in Fig. 4 in-

Table 1. Structures and blocking activities of the *bis*-cationic compounds used

No	N ⁺ Me ₃ – (CH ₂) ₅ – R			No	N ⁺ Et ₃ – (CH ₂) ₅ – R		
	R	IC ₅₀ , μM	<i>n</i>		R	IC ₅₀ , μM	<i>n</i>
I	–N ⁺ Me ₃	5.9 ± 2.6	3	IX		2.5 ± 0.2	3
II		0.6 ± 0.1	5	X	–N ⁺ Me Et ₂	2.1 ± 0.3	5
III		1.7 ± 0.3	6	XI	–N ⁺ Me ₂ i-Pr	2.0 ± 0.5	4
IV	–N ⁺ Me ₂ Et	3.2 ± 0.7	3	XII		74.0 ± 16.0	3
V	–N ⁺ Me ₂ i-Pr	1.6 ± 0.2	4	XIII	–N ⁺ Et ₃	79.0 ± 7.0	4
VI	–N ⁺ H i-Pr ₂	0.8 ± 0.2	3	XIV		36.0 ± 1.4	3
VII	–N ⁺ Me i-Pr ₂	0.12 ± 0.02	5	XV	–N ⁺ Me ₂ n-Pr	16.5 ± 4.4	3
VIII	–N ⁺ Et ₃	1.7 ± 0.4	5				

R, a variable cationic head; IC₅₀, a half-effective concentration of the blocking compound; *n*, numbering of cells.

Table 2. Binding rate constants for fast (k^*_{+Bf}) and slow EPSC components (k^*_{+Bs}) in rat SCG neurons

Blocking compounds	k^*_{+Bf} (10 ⁶ M ⁻¹ sec ⁻¹)	<i>n</i>	k^*_{+Bs} (10 ⁶ M ⁻¹ sec ⁻¹)	Blocking activity (1/IC ₅₀ , M ⁻¹)
VII	51.25 ± 3.74	3	10.37 ± 2.32	8.3 ± 1.4
II	27.82 ± 2.57	5	7.28 ± 1.35	1.67 ± 0.28
IV	5.87 ± 2.08	4	1.88 ± 0.45	0.31 ± 0.07
I	2.88 ± 0.54	5	0.63 ± 0.12	0.17 ± 0.08
XV	1.40 ± 0.53	3	0.40 ± 0.12	0.061 ± 0.016
XIII	0.71 ± 0.21	3	0.14 ± 0.03	0.013 ± 0.001

cludes contributions from different compounds; the compounds VII (64.8%), II (23.1%), III (2.5%), V (2.4%), VIII (2.2%), and XI (1.4%) contributed most significantly.

In the case of the second approach, correlation between the k^*_{+Bf} and k^*_{+Bs} values listed in Table 2, on the one hand, and the MPS probability on the other, was calculated for each MPS. Figure 5 shows correlation coefficients obtained, as plotted against the corresponding MPSs. Only one peak corresponding to a correlation coefficient of 0.95 is statistically significant ($P > 0.99$), and this peak is reached at the MPS equal to 11.8 Å, both for fast and slow EPSC components. This peak is similar to that found with the first approach.

As statistically significant correlation coefficient

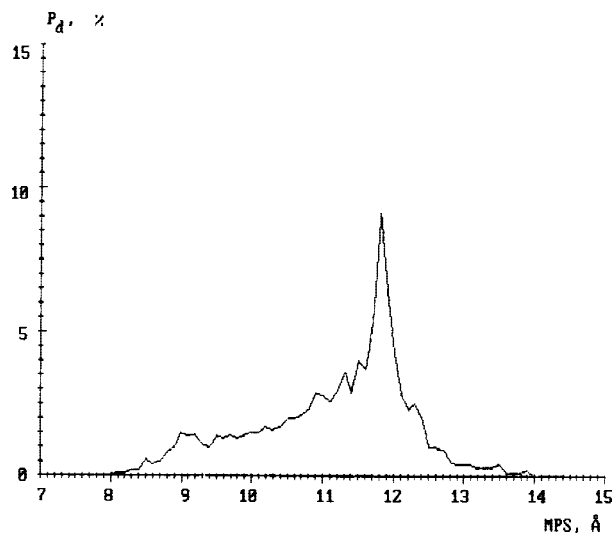


Fig. 4. Difference (P_d) between the weighted and non-weighted MPS probability spectra calculated for all the 15 blocking compounds tested (see Table 1). To obtain the weighted MPS probability spectrum, the non-weighted MPS probability spectrum of each compound was multiplied by a relative blocking activity ($1/IC_{50}$) of the compound. The sum of P_d for all MPS equals 100%.

was not observed for the MPSs smaller or larger than 11.8 Å, the blocking effect appears to be due to interaction of the blocking molecules with the channel wall just at the level where the channel diameter is 11.8 Å.

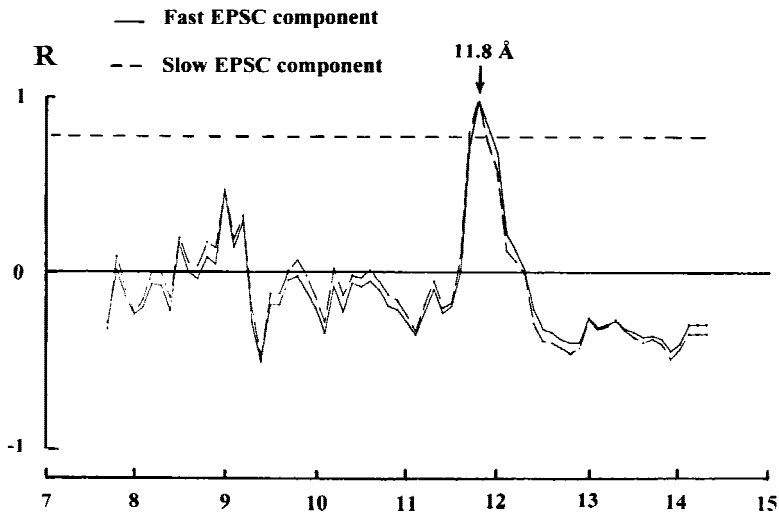


Fig. 5. Correlation between the k^*_{+Bf} (solid line) and k^*_{+Bs} (dashed line) values, on the one hand, and the MPS probabilities, on the other hand, for each MPS of the compounds listed in Table 2. Ordinate, a correlation coefficient (R). Abscissa, the MPSs. Horizontal dashed line indicates confidential level for the correlation coefficient ($P = 0.95$).

Discussion

The results obtained in this work suggest that the nAChR open-channel blockers interact with the channel at the level where the channel diameter equals 11.8 Å. This is a new channel area, not described in the previous studies using a similar approach, in which the blockers were found to interact at the channel level resembling a 6.1×8.3 Å or 5.5×6.4 Å rectangle (Zhorov et al., 1991; Brovtsyna et al., 1996). This new area was not found in the earlier studies probably because the channel diameters were tested within a relatively narrow range (from 5.4 to 9 Å: Zhorov et al., 1991, Fig. 2). The channel dimensions within this range, although wide enough to accommodate a single cationic head of the bis-ammonium compound oriented perpendicularly to the neuronal membrane, was not large enough to accommodate the MPS of the compounds at *any* orientation relative to neuronal membrane; thus, the approach used in the early studies allowed the measurement of the dimensions of only a relatively narrow and deep channel portion. An extended scale of MPS measurements used in the present work (from 7.7 to 14.6 Å) allowed us to study the channel portion of a larger diameter.

The channel diameter 11.8 Å obtained at present is consistent with those found by independent experimental methods. The studies of a permeability of nAChR channels in rat myotubes to monovalent and divalent cations suggested that the cations interact with the channel at the end of the channel vestibule near its narrow region, where the channel diameter equals 12 Å (Dani & Eisenman, 1987). According to the results obtained with electron microscopy, the diameter of the *Torpedo* nAChR channel near its entrance is slightly less than 18 Å (Unwin, 1993, 1995); therefore, the channel portion we studied is probably located somewhat deeper than the entrance.

Our results show that the decay of the EPSC recorded from rat superior cervical ganglion is bi-exponential. Similar bi-exponential decays were observed in the submandibular ganglia of the rat (Rang, 1981) and mouse (Yawo, 1989), and were interpreted as an indication that two different subtypes of nAChRs were activated. It has been generally accepted that the EPSC decay time constant is equal to a mean duration of the burst of single channel openings (*see* Colquhoun & Hawkes, 1983; Derkach et al., 1987; Adams & Nutter, 1992). Thus, it is likely that the two nAChR subtypes differ in the nAChR channel kinetics.

The fact that the peak of correlation between k^*_{+Bf} and k^*_{+Bs} , on the one hand, and the MPS probabilities, on the other hand, corresponds to a channel diameter of 11.8 Å (Fig. 5), suggests that in both nAChR subtypes the open-channel blockers bind at the channel level of 11.8 Å diameter. The data obtained are consistent with the single binding site model which was recently proposed for the interaction of monovalent and divalent cations with the nAChR channels in rat myotubes (Dani & Eisenman, 1987). At the same time, in each neuron the k^*_{+Bf} is markedly different from k^*_{+Bs} for each blocking compound tested, suggesting that even the nAChR subtypes within a single neuron may differ in terms of chemical structure that binds the blocking agents. This suggestion is consistent with recent concepts on subcellular compartmentalization, within a single neuron, of the various nAChR subtypes (for review see Vidal & Changeux, 1996).

The question arises what is the structure in the nAChR molecule that binds the open channel blockers used in our experiments. The nAChRs in the neurons of the rat superior cervical ganglion are thought to be composed of $\alpha 3$, $\alpha 5$, $\alpha 7$, $\beta 2$, $\beta 4$ (Role, 1992; Mandeleus et al.; De Koninck & Cooper, 1995; *see* Albuquerque et al., 1995; Lindstrom, 1996; Lindstrom et al., 1995), and

α 4-1 subunits (Rust et al., 1994), forming different nAChR receptor subtypes. In particular, α 3 and β 4 subunits were found to be most common in the rat SCG. In most recent immunochemical studies, α 3, α 5, and α 7 subunits were found in rat SCG (M.V. Skok, *personal communication*). The nAChR ionic channel is thought to be lined by the M2 membrane-spanning domains of each subunit (Imoto et al., 1988), with few rings of negatively charged amino acids and uncharged polar amino acids serine and threonine determining the channel interaction with divalent cations (Imoto et al., 1988, 1991; Bertrand et al., 1993; Vidal & Changeux, 1996) and with most noncompetitive and open-channel blockers (Leonard et al., 1988; Revah et al., 1990). Different α subunits differ in chemical structure of the negatively charged rings (*see, e.g., Skok, 1992*), which may provide a base for the differences between $k^*_{+B\beta}$ and $k^*_{+B\alpha}$ in the same neuron found in this work. In particular, there is a great diversity among the α 3, α 4, α 5 and α 7 subunits in the amino residues at 276 and 274 positions (*see Lindstrom, 1996, Fig. 3*), which are close to the outer rings crucial for interaction of the channel with divalent cations (*see Vidal & Changeux, 1996*). At the same time, the two different nAChR subtypes proposed by the present study do not differ with respect to the channel diameter at the channel level at which the open channel blockers that were tested at this time carry out their binding.

This work has been supported by the International Science Foundation (USA) and by the Basic Research Foundation (Russia).

References

- Adams, P.R. 1976. Drug blockade of open end-plate channels. *J. Physiol.* **260**:531–552
- Adams, D.J., Nutter, T.J. 1992. Calcium permeability and modulation of nicotinic acetylcholine receptor-channel in rat parasympathetic neurons. *J. Physiol.* **86**:67–76
- Albuquerque, E.X., Pereira, E.F.R., Castro, N.G., Alkondon, M., Reinhardt, S., Schreder, H., Maelicke, A. 1995. Nicotinic receptor function in the mammalian central nervous system. *Ann. New York Acad. Sci.* **757**:48–72
- Ascher, P., Large, W.A., Rang, H. 1979. Studies on the mechanism of action of acetylcholine antagonists on rat parasympathetic ganglion cells. *J. Physiol.* **295**:139–170
- Bertrand, D., Galzi, J.-L., Devillers-Thiery, A., Bertrand, S., Changeux, J.-P. 1993. Stratification of the channel domain in neurotransmitter receptors. *Current Opinion in Cell Biology* **5**:688–693
- Boulter, J., O'Shea-Greenfield, A., Duvoisin, R., Connolly, J., Wada, E., Jensen, A., Ballivet, M., Gardner, P.D., Deneris, E., McKinnon, D., Heinemann, S., Patrick, J. 1990. Alpha3, Alpha5 and Beta4: Three members of the rat neuronal nicotinic acetylcholine receptor-related gene family form a gene cluster. *J. Biol. Chem.* **265**:4472–4482
- Brovtsyna, N.B., Tikhonov, D.B., Gorbunova, O.B., Gmiro, V.E., Serduk, S.E., Lukomskaia, N.Y., Magazanik, L.G., Zhorov, B.S. 1996. Architecture of the neuronal nicotinic acetylcholine receptor ion channel at the binding site of bis-ammonium blockers. *J. Membrane Biol.* **152**:77–87
- Changeux, J.P., Galzi, J.L., Devillers-Thiery, A., Bertrand, D. 1992. The functional architecture of the acetylcholine nicotinic receptor explored by affinity labeling and site-directed mutagenesis. *Quarterly Rev. Biophys.* **25**:395–432
- Colquhoun, D., Hawkes, A.G. 1983. The principles of the stochastic interpretation of ion-channel mechanisms. *In: Single-Channel Recording*, B. Sakmann and E. Neher, Editors, pp. 135–175, Plenum Press, New York & London
- Colquhoun, D., Ogden, D.C., Mathie, A. 1987. Nicotinic acetylcholine receptors of nerve and muscle: functional aspects. *TIPS* **8**:465–472
- Dani, J.A., Eisenman, G. 1987. Monovalent and divalent cation permeation in acetylcholine receptor channels. *J. Gen. Physiol.* **89**:959–983
- De Koninck, P., Cooper, E. 1995. Differential regulation of neuronal nicotinic ACh receptor subunit genes in cultured neonatal rat sympathetic neurons: specific induction of α_7 by membrane depolarization through a Ca^{2+} /calmodulin-dependent kinase pathway. *J. Neurosci.* **15**:7966–7978
- Derkach, V.A., North, R.A., Selyanko, A.A., Skok, V.I. 1987. Single channels activated by acetylcholine in rat superior cervical ganglion. *J. Physiol.* **388**:141–151
- Dwyer, T.M., Adams, D.J., Hille, B. 1980. The permeability of the end-plate channel to organic cations in frog muscle. *J. Gen. Physiol.* **75**:469–492
- Giles, I.G. 1985. Microcomputer molecular graphics. *In: Microcomputers in Neurosciences*, G.A. Kerkut, editor, pp. 202–205, Clarendon Press, Oxford
- Gurney, A.M., Rang, H.P. 1984. The channel-blocking action of methonium compounds on rat submandibular ganglion cells. *Br. J. Pharmacol.* **82**:623–642
- Hille, B. 1984. *Ionic Channels in Excitable Membranes*. Sinauer Associates, Sunderland, MA
- Imoto, K., Bush, H., Sakmann, B., Mishina, M., Konno, T., Nakai, J., Bujo, H., Mori, Y., Fukuda, K., Numa, Sh. 1988. Rings of negatively charged amino acids determine the acetylcholine receptor channel conductance. *Nature* **335**:645–648
- Imoto, K., Konno, T., Nakai, J., Wang, F., Mishina, M., & Numa, Sh. 1991. A ring of uncharged polar amino acids as a component of channel constriction in the nicotinic acetylcholine receptor. *FEBS Lett.* **289**:193–200
- Leonard, R.J., Labarca, C.G., Charnett, P., Davidson, N., Lester, H. 1988. Evidence that the M2 membrane-spanning region lines the ion channel pore of the nicotinic receptor. *Science* **242**:1578–1581
- Lindstrom, J. 1996. Neuronal nicotinic acetylcholine receptors. *In: Ion Channels*, T. Narahashi, Editor, pp. 377–449, Plenum Press, New York
- Lindstrom, J., Anand, R., Peng, X., Gerzanich, V., Wang, F., Li, Y. 1995. Neuronal nicotinic receptor subtypes. *Ann. New York Acad. Sci.* **757**:100–116
- Luetje, C.W., Patrick, J. 1991. Both α - and β -subunits contribute to the agonist sensitivity of neuronal nicotinic acetylcholine receptors. *J. Neurosci.* **11**:837–845
- Mandeleus, A., Pie, B., Deneris, E.S., Cooper, E. 1994. The developmental increase in ACh current densities on rat sympathetic neurons correlates with changes in nicotinic ACh receptor α -subunit gene expression and occurs independent of innervation. *J. Neurosci.* **14**:2357–2364
- Rang, H. 1981. The characteristics of synaptic currents and responses to acetylcholine in rat submandibular ganglion cells. *Br. J. Pharmacol.* **75**:151–158
- Revah, F., Galzi, J.-L., Giraudat, J., Haumont, P.-Y., Lederer, F., Changeux, J.-P. 1990. The noncompetitive blocker [3 H]chlorpromazine labels three amino acids of the acetylcholine receptor γ -subunit: implications for the α -helical organization of regions MII and for

- the structure of the ion channel. *Proc. Natl. Acad. Sci. USA* **87**:4675–4679
- Role, L.W. 1992. Diversity in primary structure and function of neuronal nicotinic acetylcholine receptor channels. *Curr. Opin. Neurobiol.* **2**:254–262
- Rust, G., Burgender, J.-M., Lautenburg, T.E., Cachelin, A.B. 1994. Expression of neuronal nicotinic acetylcholine receptor subunit genes in the rat autonomic nervous system. *Europ. J. Neurosci.* **6**:478–485
- Skok, V.I. 1992. Molecular mechanisms of open-channel blockade in nicotinic acetylcholine receptors of autonomic ganglia neurons. *Ca. J. Physiol. Pharmacol.* **70**:S78–S85
- Skok, V.I., Selyanko, A.A., Derkach, V.A. 1983. Channel-blocking activity is a possible mechanism for a selective ganglionic blockade. *Pfluegers Arch.* **398**:169–171
- Skok, V.I., Selyanko, A.A., Derkach, V.A. 1989. *Neuronal Acetylcholine Receptors*. Plenum Press, New York-London
- Skok, V.I., Voitenko, S.V., Kurenniy, D.E., Brovtsyna, N.B., Gmiro, V.E., Kertser, S.L. 1995. The ionic channel of neural nicotinic acetylcholine receptors is funnel-shaped. *Neuroscience* **67**:933–939
- Steinbach, J.H., Ifune, C. 1989. How many kinds of nicotinic acetylcholine receptor are there? *Trends Neurosci.* **12**:3–6
- Unwin, N. 1993. Nicotinic acetylcholine receptor at 9 Å resolution. *J. Mol. Biol.* **229**:1101–1124
- Unwin, N. 1995. Acetylcholine receptor channel imaged in the open state. *Nature* **373**:37–45
- Vidal, C., Changeux, J.-P. 1996. Neuronal nicotinic acetylcholine receptors in the brain. *NIPS* **11**:202–207
- Vinter, J.G., Davis, A., Saunders, M.R. 1987. Strategic approaches to drug design. I. An integrated software framework for molecular modelling. *Journal of Computer Aided Molecular Design* **1**:31–51
- Voitenko, S.V., Bobryshev, A.U., Skok, V.I. 1993. Effect of tetraethylammonium on nicotinic acetylcholine receptors in rat sympathetic ganglion neurones. *Molecular Neuropharmacol.* **3**, 153–160
- Yawo, H. 1989. Rectification of synaptic and acetylcholine currents in mouse submandibular ganglion cells. *J. Physiol.* **417**:307–322
- Zhorov, B.S., Brovtsyna, N.B., Gmiro, V.E., Lukomskaya, N. Ya., Serdyuk, S.E., Potapyeva, N.N., Magazanik, L.G., Kurenniy, D.E., Skok, V.I. 1991. Dimensions of the ion channel in neuronal nicotinic acetylcholine receptor as estimated from analysis of conformation-activity relationships of open-channel blocking drugs. *J. Membrane Biol.* **121**:119–132